Journal of Translational Medicine

RESEARCH

Open Access

SIRT6 prevent chronic cerebral hypoperfusion induced cognitive impairment by remodeling mitochondrial dynamics in a STAT5-PGAM5-Drp1 dependent manner

Yong Du[1†], Jiaqing He[2†], Yanni Xu[1†], Xun Wu[1], Hongbo Cheng[3], Jiegang Yu[3], Xiaoliang Wang[3], Yaqing An[4], Yang Wu[3*] and Wei Guo[1*]

Abstract

Vascular dementia (VaD) is a prevalent form of dementia resulting from chronic cerebral hypoperfusion (CCH). However, the pathogenic mechanisms of VaD and corresponding therapeutic strategies are not well understood. Sirtuin 6 (SIRT6) has been implicated in various biological processes, including cellular metabolism, DNA repair, redox homeostasis, and aging. Nevertheless, its functional relevance in VaD remains unexplored. In this study, we utilized a bilateral common carotid artery stenosis (BCAS) mouse model of VaD to investigate the role of SIRT6. We detected a significant decrease in neuronal SIRT6 protein expression following CCH. Intriguingly, neuron-specific ablation of Sirt6 in mice exacerbated neuronal damage and cognitive deficits after CCH. Conversely, treatment with MDL-800, an agonist of SIRT6, effectively mitigated neuronal loss and facilitated neurological recovery. Mechanistically, SIRT6 inhibited excessive mitochondrial fission by suppressing the CCH-induced STAT5-PGAM5-Drp1 signaling cascade. Additionally, the gene expression of monocyte SIRT6 in patients with asymptomatic carotid stenosis showed a correlation with cognitive outcomes, suggesting translational implications in human subjects. Our findings provide the first evidence that SIRT6 prevents cognitive impairment induced by CCH, and mechanistically, this protection is achieved through the remodeling of mitochondrial dynamics in a STAT5-PGAM5-Drp1-dependent manner.

Keywords Chronic cerebral hypoperfusion, SIRT6, Cognitive impairment, Drp1, Mitochondrial dynamics

†Yong Du, Jiaqing He, Yanni Xu these authors contributed equally to this work.

*Correspondence:
Yang Wu
28704926@hebmu.edu.cn
Wei Guo
18729985168@163.com

[1]Department of Neurosurgery, Tangdu Hospital, Air Force Medical University, Xi'an, Shaanxi 710032, China
[2]Department of Neurosurgery, Xi'an Medical University, Xi'an, Shaanxi 710032, China
[3]Department of Neurosurgery, The second Hospital of Hebei Medical University, Shijiazhuang, Hebei 050000, China
[4]Department of Emergency, The second Hospital of Hebei Medical University, Shijiazhuang, Hebei 050000, China

Introduction

Vascular dementia (VaD), resulting from chronic cerebral hypoperfusion (CCH), is the second most prevalent form of dementia, accounting for approximately 20% of cases [1–3]. Pathological changes observed in VaD include mitochondrial damage, oxidative stress, and neuronal injury [4–6]. Understanding the underlying mechanisms of these events may facilitate the development of therapeutic interventions against VaD.

SIRT6, a member of the sirtuin family of enzymes, is involved in gene expression regulation by removing specific chemical groups, such as acetyl groups, from histone proteins [7, 8]. By modulating gene expression, SIRT6 impacts crucial cellular functions, including DNA repair, energy metabolism, and aging [9–11]. Notably, SIRT6 has been identified as a crucial target for age-related brain injuries. For example, endothelial SIRT6 has been shown to mitigate secondary brain injury and promote neurological recovery through protecting against blood-brain barrier damage [12]. Additionally, SIRT6 has been implicated in the protection against neurodegenerative diseases including Parkinson's and Alzheimer's disease, through its ability to safeguard neurons against oxidative stress and reduce inflammation [13, 14]. Therefore, unraveling the functions and mechanisms of SIRT6 may offer valuable insights into potential therapeutic strategies for central nervous system (CNS) disorders. However, the specific role of SIRT6 in CCH-induced cognitive impairment remains unexplored.

Mitochondria, the crucial generators of adenosine triphosphate (ATP) via oxidative phosphorylation, play a pivotal role in brain function [15–17]. Impaired ATP production, accumulation of ROS, and disrupted mitochondrial dynamics are common manifestations of mitochondrial damage in this context of CCH [18–20]. These alterations contribute significantly to neuronal dysfunction, ultimately leading to cognitive decline. Notably, the intricate interplay between mitochondrial dynamics and function has recently gained considerable attention [21–24]. Fusion and fission processes intricately modulate the morphology and function of mitochondria, with Drp1 primarily regulating mitochondrial fission, and OPA1, MFN1, and MFN2 governing mitochondrial fusion [25, 26]. Dysregulation of fusion and fission events in the brain has been implicated to involve in the pathogenesis of cognitive impairment-related disorders [27–30]. Consequently, modulating mitochondrial dynamics has emerged as a promising strategy for restoring mitochondrial function, mitigating oxidative stress, and promoting neuronal well-being.

In the study, we aimed to explore the potential role of SIRT6 in the progression of VaD and uncovered the underlying molecular mechanisms, which may shed light on the establishment of new therapeutic strategies for VAD.

Materials and methods

Animals and ethics

All animal experimental procedures were approved by the animal experiment center of Fourth Military Medical University (IACUC-20220574) and were conducted in accordance with the guidelines outlined in the National Institutes of Health Guide for the Care and Use of Laboratory Animals. C57/6BJ mice were obtained from the Fourth Military Medical University. Neuronal-specific Sirt6 knockout mice were generated through crossbreeding Sirt6-Floxed mice with Map2-CreERT2 mice (both obtained from the Shanghai Model Organisms Center), followed by tamoxifen treatment (dosage: 75 mg/kg, 5 consecutive days). All mice were housed in a controlled environment with a constant temperature of 27 °C, humidity of 60%, and a 12-hour light/dark cycle. The mice were given free access to water and food. And at the corresponding time point after experimental processing, mouse was sacrificed by an overdose of 2% pentobarbital sodium and brain tissues were collected for further analysis.

In the first section, we utilized 36 wild-type C57BL/6J mice (6 mice each from the Sham group, BCAS-3d group, BCAS-7d group, BCAS-14d group, BCAS-28d group, and BCAS-60d group) for western blot analysis to determine the protein expression of SIRT6 following BCAS. And we used 12 wild-type C57BL/6J mice (6 mice each from the Sham group and BCAS-28d group) for immunofluorescence staining to determine the spatialization of SIRT6. In the second section, experiments encompassed nissl staining, transmission electron microscope, and western blot each utilized 24 mice (6 mice each from $Sirt6^{fl/fl}$ + Sham group, $Sirt6^{fl/fl}$ + BCAS group, $Sirt6^{CKO}$+Sham group, and $Sirt6^{CKO}$+BCAS group). Neurobehavioral tests involved 48 mice (12 mice each from $Sirt6^{fl/fl}$ + Sham group, $Sirt6^{fl/fl}$ + BCAS group, $Sirt6^{CKO}$+Sham group, and $Sirt6^{CKO}$+BCAS group). In the third section, experiments involving nissl staining, transmission electron microscope, and western blot each utilized 18 wild-type C57BL/6J mice (6 mice each from the Sham group, BCAS group, and BCAS+MDL-800 group). Neurobehavioral tests utilized 36 mice (Sham group, BCAS group, and BCAS+MDL-800 group).

Establishment of the bilateral common carotid artery stenosis (BCAS) mouse model

The BCAS model was employed to induce VaD [31]. Briefly, mice were anesthetized with 0.3% pentobarbital sodium, and the right common carotid artery was then carefully separated and fully exposed. Subsequently, a microcoil with an internal diameter of 0.18 mm was

wrapped around the artery. The same operations were performed on the left common carotid artery. Data obtained from mice that did not survive the procedure were excluded from analysis.

Morris water maze (MWM) experiment

MWM experiment was used to evaluate spatial learning and memory abilities, and was conducted in accordance with previously published methods [32]. In brief, the MWM apparatus consisted of a circular water tank made of black plastic, with a diameter of 120 centimeters and filled with water to a depth of 45 centimeters. White ink was added to render the water opaque. An escape platform with a diameter of 10 cm, intentionally concealed beneath the water surface, was consistently positioned at the center of the designated "target" quadrant throughout all phases of the behavioral training, serving as the sole escape location for the mice. During the learning period, the mice were allowed to freely navigate the maze until they successfully reached the hidden platform. In cases where the mice failed to locate the platform within a 1-minute period, they were manually guided to it for a duration of 10 s. When the mouse successfully reached the platform or when the 1-minute time limit was reached, the trial was ended and the escape latency was record. The learning period spans five consecutive days and was utilized to evaluate the spatial learning ability of the mice. On day 6, the escape platform was removed and the probe trial was conducted to assess the spatial memory ability of the mice. Each mouse was allowed to swim freely for 1 min. The number of platform crossings and the time spent in the target quadrant were quantified and used as indicators of spatial memory performance.

Nissl staining

Upon anesthesia, the brains of the mice were gently extracted and fixed in a 4% paraformaldehyde solution overnight. After dehydrated in 30% sucrose solutions for 24 h, the brain tissues were embedded in paraffin and cut into coronal sections with a thickness of 15 μm with a Leica RM2255 microtome. Finally, these brain sections were stained using a Nissl staining kit (Solarbio, Beijing, China) following the instructions provided by the manufacturers.

Transmission electron microscope

Transmission electron microscopy was performed according to the methods described previously [33]. The brain tissues were dissected and treated with electron microscope fixative solution at 4 °C for 4 h. After being washed three times with PBS, the tissues were post-fixed in 1% OsO4 at 4 °C for 1 h and washed again with PBS three times. Subsequently, the tissues were dehydrated in a series of ethanol solutions (30%, 50%, 70%, 80%, 90%, and 100%) for 15–20 min each, followed by a 20-minute incubation in acetone. The tissues were then permeated in a mixture of acetone and resin (1:1) for 1 h at 25 °C, and subsequently transferred to a mixture of acetone and resin (1:3) overnight. Tissues were carefully placed near the embedded blocks, avoiding the dorsal rim area, and stained with uranyl acetate and alkaline lead citrate for 15 min. Finally, tissues were observed using a JEM-1230 TEM (JEOL, Tokyo, Japan), and images were captured using a side-inserted BioScan Camera (Veleta, EMSIS GmbH, Germany).

Immunofluorescence

Immunofluorescence was performed as previously described [34]. Briefly, tissue sections with a thickness of 15 μm were obtained as mentioned above in Nissl staining. Brain sections were permeabilized with 0.2% Triton X-100 for 15 min, followed by the incubation with 3% bovine serum albumin for 30 min. Subsequently, the sections were incubated overnight at 4 °C using the following primary antibodies: rabbit anti-Sirt6 (1:50, CST, D8D12) and goat anti-Neuron (1:500, Invitrogen, PA5-143586). After rinsing the sections in PBS (3×5 min), they were incubated with species-compatible fluorescent secondary antibodies for 2 h. This step is performed in a dark environment. Finally, the sections were stained with DAPI and observed under a fluorescent microscope.

Western blots

Tissues were homogenized through sonication in 200 μL of RIPA buffer, and the protein concentration was measured using a BCA kit following to the instructions. Equal amounts of proteins were separated by SDS-PAGE gels and transferred onto PVDF membranes (Millipore, USA) using the semi-dry transfer method. Following a 2-hour blocking period with 5% nonfat dried milk, the membranes were subjected to an overnight incubation at 4 °C with primary antibodies, including anti-Sirt6 (1:1000, CST), anti-STAT5 (1:1000, CST), anti-PGAM5 (1:1000, Abcam), anti-DRP1 (1:1000, Abcam), and anti-phospho-DRP1-Ser637 (1:1000, Abcam) antibodies. Subsequently, the membranes were incubated for 1 h with secondary antibodies that were compatible with the species used. The specific protein bands were detected using a Bio-Rad Gel Doc Image.

Measurement of mitochondrial function

Measurement of ATP production and mitochondrial electron transport chain (ETC) complex activities in brain tissues were performed as described [35]. Elisa assays were performed to measure ATP content (BC0300, Solarbio) and mitochondrial ETC (I-II) complex (BC0515, BC3230, Solarbio) activities according to the manufacturer's instructions.

Patients

Peripheral blood samples were obtained from patients diagnosed with asymptomatic carotid stenosis at Tangdu Hospital of Fourth Military Medical University, and these samples were utilized to explore the relationship between SIRT6 expression and the cognitive prognosis after carotid revascularization surgery. The human research conducted in this investigation was approved by the Ethics Committee of Tangdu Hospital, the Air Force Military Medical University (TD-K202201-10). Informed consent was obtained from the participants or their legally authorized representatives. The study included a total of 164 patients with asymptomatic carotid stenosis who exhibited cognitive impairments, as assessed using the Montreal Cognitive Assessment (MoCA) scale. The inclusion criteria comprised the following: unilateral internal carotid artery stenosis ≥ 70% based on CT/MR angiography or unilateral internal carotid artery stenosis ≥ 60% confirmed by angiography, with the contralateral side exhibiting no stenosis or stenosis < 50%; no history of stroke or transient ischemic attack; absence of ischemic lesions or scattered chronic ischemic lesions on cerebral MRI examination; a > 30% relative decrease in regional cerebral blood flow (rCBF) on CT perfusion imaging in the affected hemisphere. Exclusion criteria were as follows: the presence of neurological symptoms or signs, a National Institutes of Health Stroke Scale (NIHSS) score > 1; degenerative changes in the nervous system or cognitive dysfunction caused by other etiologies, such as cranial trauma, neurological tumors, infections, metabolic disorders, normal pressure hydrocephalus, hypothyroidism, etc.; patients with severe psychiatric disorders that hinder communication; the presence of severe organ dysfunction (including liver, kidney, digestive, respiratory, circulatory, endocrine, immune, and hematological diseases) or other diseases that researchers deemed to affect safety assessment; patients with concurrent epilepsy, Parkinson's disease, Huntington's disease, or a history of specific medication use or confirmed alcohol or drug dependence within the past 6 months; patients with intracranial aneurysms, arteriovenous malformations, dissection aneurysms, or suspected non-atherosclerotic diseases such as arteritis; subjects who refused follow-up. Venous blood samples were collected, and peripheral blood mononuclear cells (PBMCs) were isolated using differential centrifugation with Histopaque-1077 (Sigma Aldrich), as previously described [36]. The primary outcome measure was the neurologic function at 6 months after carotid revascularization, which was assessed using the MoCA. Functional outcomes were categorized as unfavorable if the MoCA score was less than 21, and as favorable if the score was greater than or equal to 21.

Statistical analyses

Data are expressed as mean ± standard deviation (SD). All statistical analyses were performed using GraphPad Prism software. Statistical comparison of the means between two groups of normal distribution was conducted using the Student's t-test (two-tailed). Differences in means among multiple groups were analyzed using one or two-way ANOVA followed by the Bonferroni post hoc correction. A probability value (P) below 0.05 was considered statistically significant.

Results

Decreased SIRT6 expression following CCH

To explore the potential association between SIRT6 and cognitive impairment in VaD, we initially established a mouse model of chronic cerebral hypoperfusion (CCH) through bilateral common carotid artery stenosis (BCAS). Prior to and after the BCAS surgery, cerebral blood flow (CBF) was measured and the results revealed a significant reduction in CBF in the BCAS groups compared to the sham group (Fig. 1A and B). Furthermore, western blot (WB) analysis demonstrated a marked decrease in SIRT6 protein expression in the hippocampus of the BCAS group compared to the sham group (Fig. 1C and D), which was also confirmed by immunofluorescent staining analysis (Fig. 1E and F). Collectively, these findings provide evidence for a decline in SIRT6 protein expression in response to CCH.

Neuron-specific Sirt6 knockout aggravates neuronal loss and cognitive deficit following CCH

We then investigated whether the decreased SIRT6 expression was associated with the cognitive impairment induced by CCH. To achieve this, we generated neuron-specific Sirt6 knockout mice using the Cre/LoxP system. Nissl staining revealed widespread neuronal loss in the hippocampus following BCAS, with a more pronounced effect observed in Sirt6 CKO mice (Fig. 2A and B). To evaluate spatial learning and memory abilities, we conducted the Morris water maze (MWM) test. The swimming pathways of mice from the sham, $Sirt6^{f/f}$+Sham, $Sirt6^{f/f}$+BCAS, Sirt6 ^{CKO}+Sham, and $Sirt6^{CKO}$+BCAS groups are depicted in Fig. 2C. Notably, all four groups exhibited similar swimming speeds, indicating comparable swimming skills (Fig. 2D) and excluding potential confounding factors that could influence performance. The results revealed a longer mean escape latency in the $Sirt6^{f/f}$+BCAS group compared to the $Sirt6^{f/f}$ group, suggesting that they had impaired spatial learning ability. In comparison to the $Sirt6^{f/f}$+BCAS group, the Sirt6 ^{CKO}+BCAS group exhibited a significantly longer mean escape latency, indicating a worsened learning ability (Fig. 2E). Consistently, during the spatial probe trial, the Sirt6 ^{CKO}+BCAS mice spent less time in the target

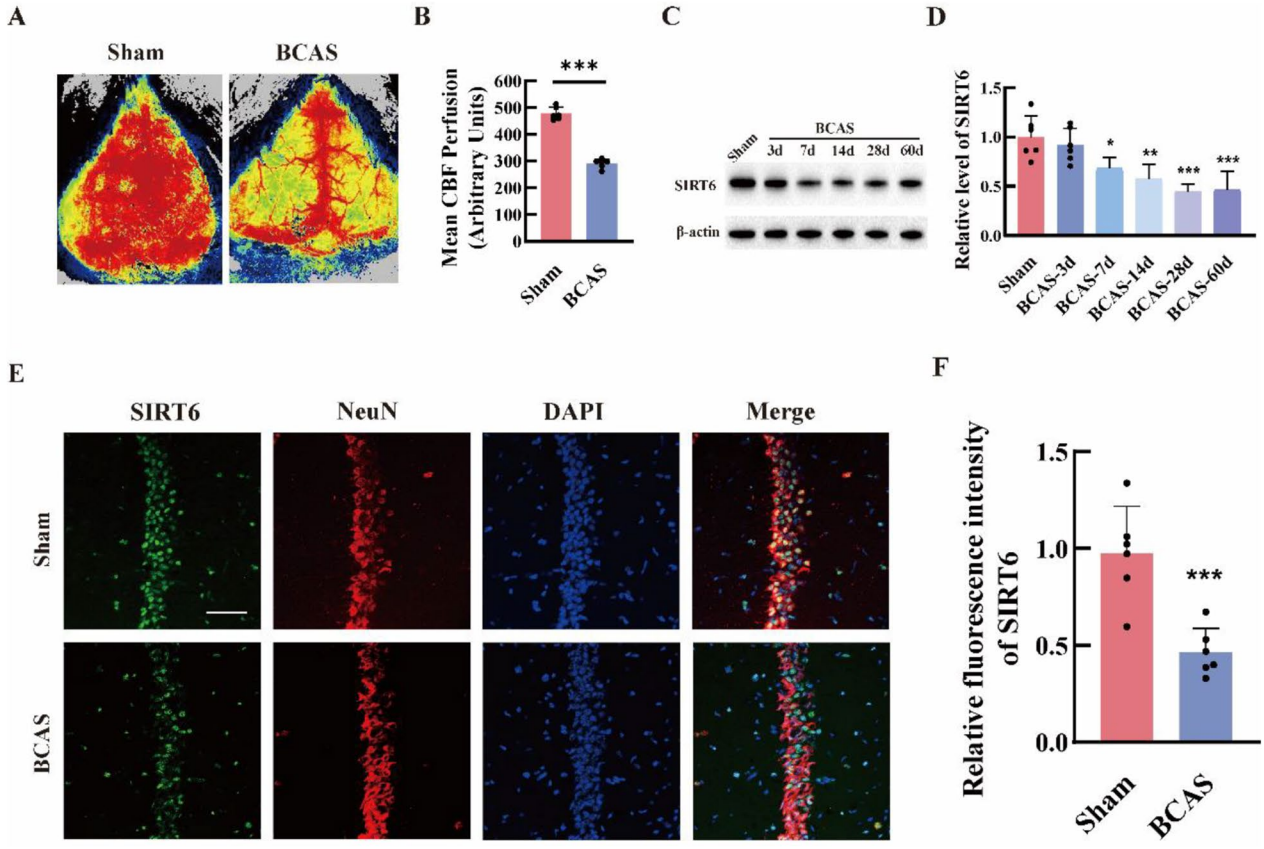

Fig. 1 Decreased protein expression of SIRT6 following chronic cerebral hypoperfusion. (**A**-**B**) Representative images (**A**) and quantification (**B**) of CBF with or without BCAS ($n=6$ per group). BCAS: bilateral common carotid artery stenosis; CBF: cerebral blood flow. (**C**-**D**) Western blot analysis of SIRT6 protein expression in hippocampus at different time points following BCAS operation in mice ($n=6$ per group). (**E**-**F**) Representative immunofluorescence staining of SIRT6 and NeuN in hippocampus at 28d following BCAS operation in mice ($n=6$ per group). Scale bars, 50 μm. Data are presented as means ± SD. $^{*}P<0.05$, $^{**}P<0.01$, $^{***}P<0.001$

quadrant and had fewer platform crossings compared to the Sirt6$^{f/f}$+BCAS group (Fig. 2F and G). These findings collectively suggest that neuron-specific Sirt6 deficiency aggravates neuronal loss and cognitive deficit in mice following CCH.

Neuron-specific Sirt6 knockout aggravates the damage of mitochondrial dynamics following CCH

To elucidate the molecular mechanisms underlying the aggravated neuronal loss and cognitive impairment in the absence of SIRT6, we investigated the impact on mitochondria. Mitochondrial damage has been implicated in the progression of VaD, and recent studies have highlighted the regulatory role of SIRT6 in mitochondrial quality control. Using transmission electron microscopy, we observed misshapen mitochondria with disrupted internal structure in the BCAS group, particularly in Sirt6 ^{CKO} mice (Fig. 3A). We further examined the modulator proteins involved in mitochondrial dynamics, including Drp1, Mfn1, Mfn2, and OPA1. Drp1 facilitates mitochondrial fission in response to various stresses by translocating from the cytoplasm to the mitochondrial membrane. Phosphorylation of Drp1 at S616 enhances its recruitment to the mitochondrial membrane, while phosphorylation at S637 hinders this process. In this study, we observed that the protein level of total Drp1 remained unchanged following BCAS in mice. However, a significant decrease in the phosphorylation level of Drp1 at S637 was evident after BCAS, particularly in Sirt6^{CKO} mice (Fig. 3B and C). Meanwhile, the levels of OPA1, Mfn1, and Mfn2 exhibited no significant changes after BCAS (Fig. 3B and C). Consequently, the heightened activities of Drp1 resulting from SIRT6 deficiency may serve as a pivotal mechanism underlying BCAS-induced mitochondrial dynamics impairment.

SIRT6 prevents damage to mitochondria by inhibiting STAT5-PGAM5-Drp1 signaling following CCH

We then investigated the therapeutic potential of the SIRT6 agonist MDL-800 in mitigating mitochondrial dynamics damage induced by CCH. Remarkably, MDL-800 treatment effectively reversed the morphological

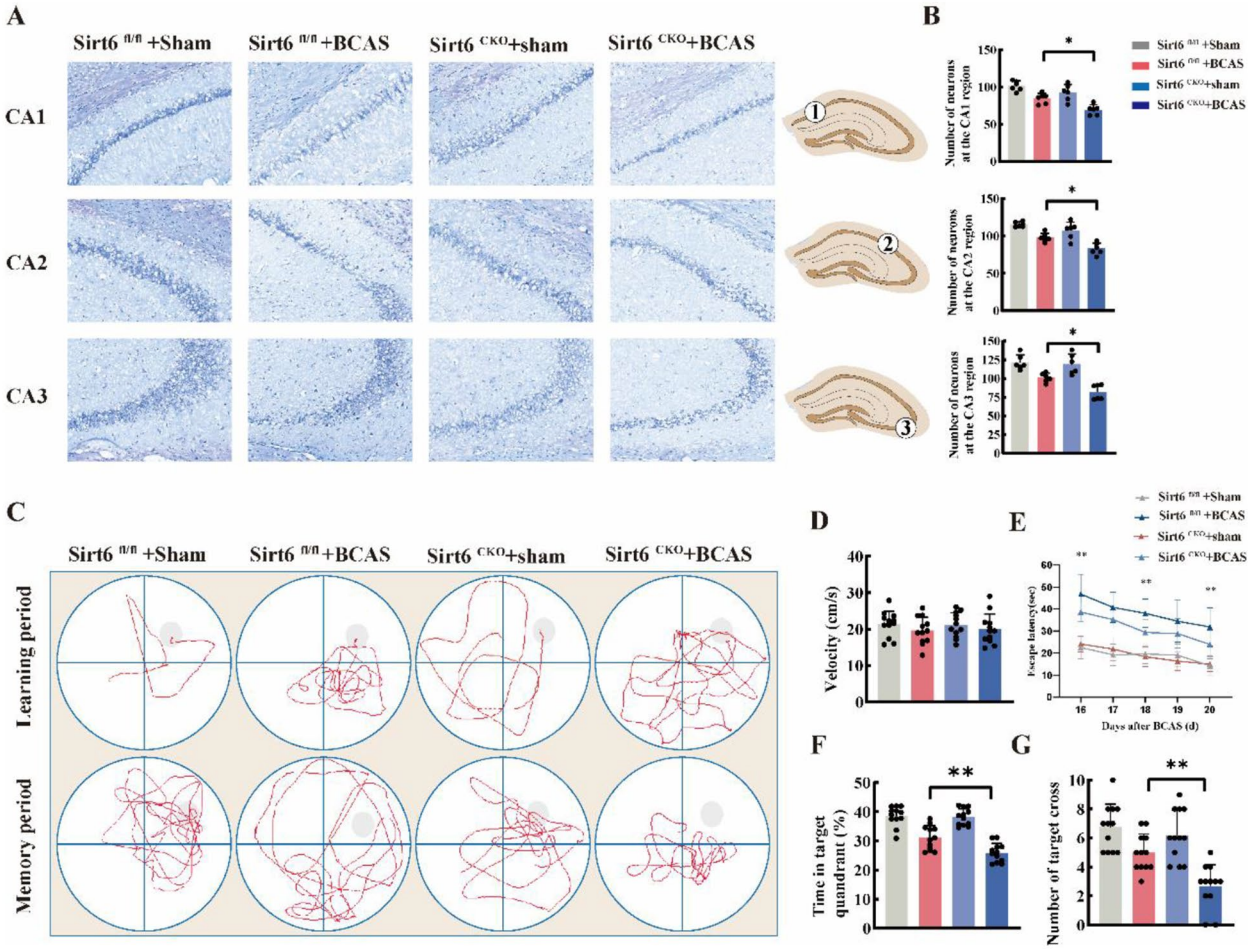

Fig. 2 Neuron-specific Sirt6 knockout aggravates neuronal loss and cognitive deficit after BCAS. (**A**-**B**) Representative images and quantification illustrating Nissl positively stained neurons in hippocampal CA1, CA2, and CA3 regions in Sirt6^{CKO} mice compared to Sirt6$^{fl/fl}$ controls following BCAS ($n=6$ per group). (**C**-**G**) The animals' learning and memory functions were assessed by the Morris water maze test. (**C**) Representative swim paths. (**D**) Latency to escape 28d-32d after BCAS. ($n=12$ per group). (**E**) The number of platform zone crossings 33d after BCAS. $n=12$/group. (**F**) The time spent on the target platform zone 33d after BCAS. $n=12$/group. ($n=12$ per group). Data are presented as means ± SD. *$P<0.05$, **$P<0.01$, ***$P<0.001$

alterations observed in the mitochondria (Fig. 4A and B). In line with this, MDL-800 treatment significantly enhanced the phosphorylation level of Drp1 at S637 (Fig. 4C and D). To elucidate the molecular mechanism by which SIRT6 regulates Drp1 phosphorylation at S637, we referred to a previous study indicating that Sirt6 can deacetylate STAT5, thereby inhibiting its translocation from the cytoplasm to the nucleus. It is known that the translocation of STAT5 to the nucleus triggers the expression of phosphoglycerate mutase family member 5 (PGAM5), a mitochondrial serine/threonine phosphatase responsible for the dephosphorylation of Drp1 at S637. As expected, we observed that the STAT5-PGAM5-Drp1 pathway was significantly activated following BCAS, but its activation was significantly inhibited upon additional MDL-800 treatment (Fig. 4C and D). These findings collectively indicate that the activation of SIRT6 promotes the restoration of mitochondrial dynamics after CCH, at least partly, by inhibiting the STAT5-PGAM5-Drp1 pathway. Concomitant with the improvement in mitochondrial morphology, we also discovered that the SIRT6 agonist alleviated mitochondrial biogenesis damage and oxidative stress after chronic cerebral hypoperfusion. Specifically, overexpression of Sirt6 facilitated the restoration of ATP production (Fig. 4E), attenuated ROS production (Fig. 4F) and promoted mitochondrial complex activities (Fig. 4G and H) following BCAS. These findings collectively indicate that the activation of SIRT6 promotes the restoration of mitochondrial dynamics and mitochondrial function after CCH, at least partly, by inhibiting the STAT5-PGAM5-Drp1 pathway.

MDL-800 alleviate neuronal loss and cognitive deficit following CCH

Next, we sought to investigate the therapeutic potential of MDL-800 treatment in mitigating the neuronal loss

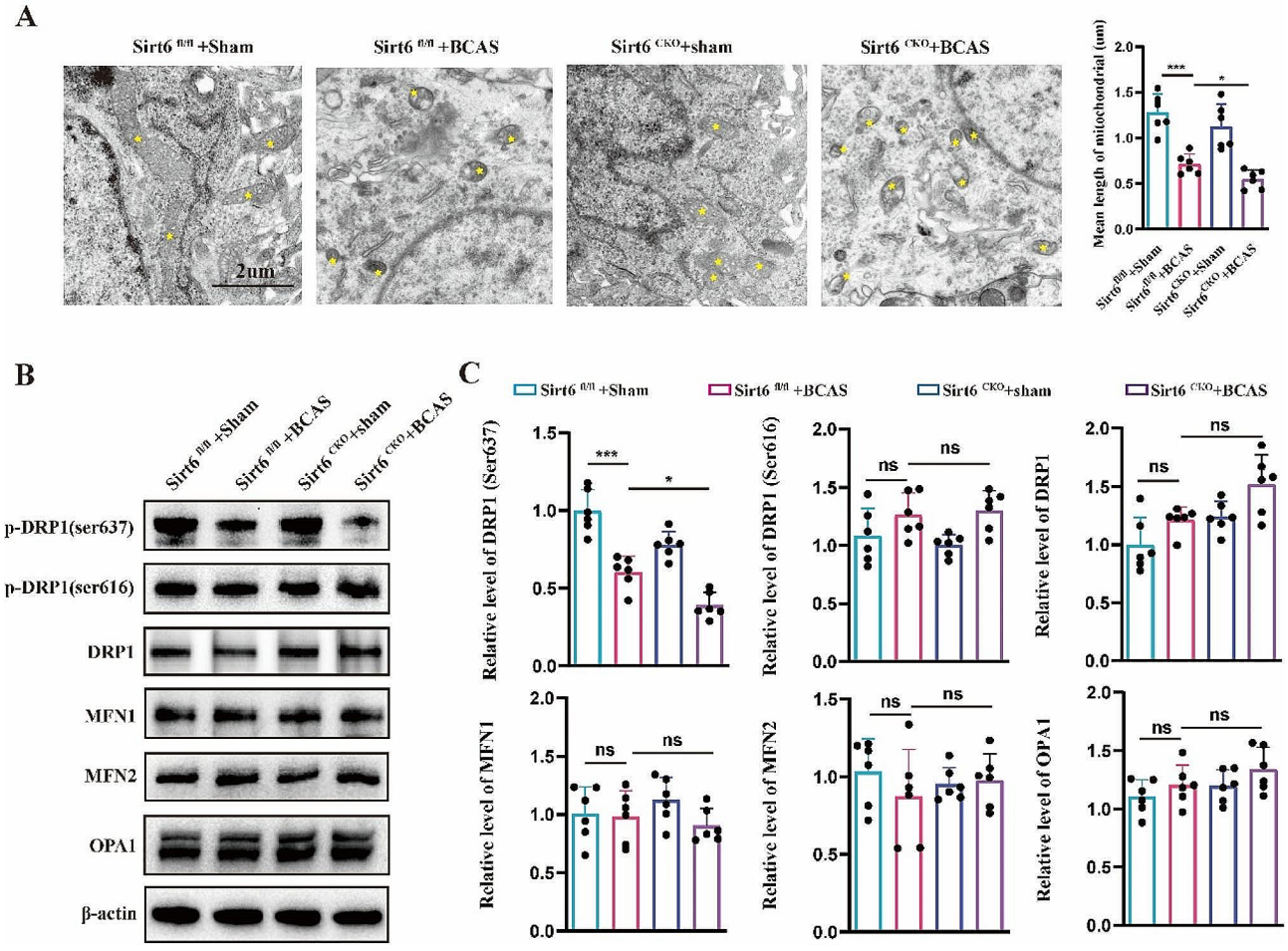

Fig. 3 Neuron-specific Sirt6 knockout aggravates the damage of mitochondrial dynamics after BCAS. (**A**) Electron microscopic images showing the ultrastructural changes in neurons from mouse brain in each group (yellow pentagram represent mitochondria). (**B**-**C**) Western blot analysis of modulator proteins of mitochondrial dynamics including Drp1, Mfn1, Mfn2 and OPA1 in mice with or without BCAS operation ($n = 6$ per group). Data are presented as means ± SD. $^{*}P < 0.05$, $^{**}P < 0.01$, $^{***}P < 0.001$

induced by CCH. To assess the efficacy of MDL-800, we performed Nissl staining, which revealed a significant attenuation of hippocampal neuron loss in mice treated with MDL-800 following BCAS (Fig. 5A and B). Furthermore, we aimed to evaluate whether MDL-800 treatment could alleviate the cognitive deficits observed in mice after BCAS. To this end, we conducted the MWM test, which revealed a prolonged mean escape latency in the BCAS group compared to the sham groups. Remarkably, administration of MDL-800 significantly reversed this cognitive impairment (Fig. 5C and E). Consistent with these findings, the spatial probe trial also demonstrated that mice receiving MDL-800 spent more time in the target quadrant and exhibited increased platform crossings compared to the BCAS group (Fig. 5F and G). Taken together, our results strongly suggest that MDL-800 treatment effectively mitigates both neuronal loss and cognitive deficits in mice experiencing CCH.

Monocyte SIRT6 gene expression in patients with asymptomatic carotid stenosis correlates with cognitive outcomes

Patients with asymptomatic carotid stenosis often coexists with cognitive impairment due to inadequate cerebral blood flow. Therefore, to validate the translational utility of our findings, we explored the associations between SIRT6 expression and cognitive outcomes in patients with asymptomatic carotid stenosis. Due to the challenges associated with acquiring brain cells from patients, we opted for peripheral blood mononuclear cells (PBMCs) as a surrogate cell type, which can be easily obtained and partially reflect molecular alterations in the brain [12, 37, 38]. A total of 164 patients were enrolled in this investigation (Table 1). Patients with favorable cognitive outcomes exhibited significantly higher Sirt6 mRNA expression in PBMCs compared to those with unfavorable cognitive outcomes (Fig. 6 A and B). Furthermore, receiver operating characteristic (ROC) curve analysis

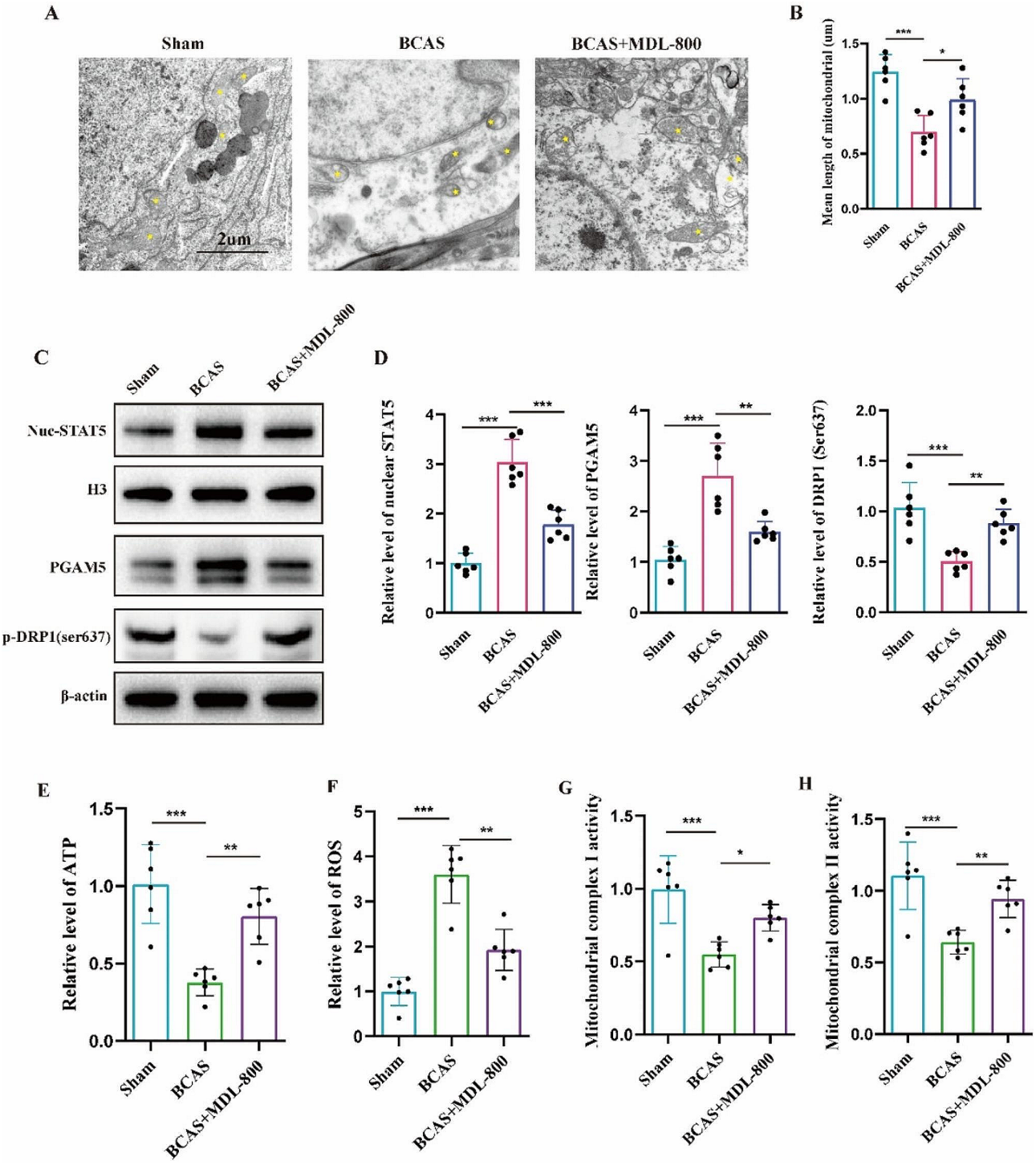

Fig. 4 SIRT6 prevents mitochondrial dynamics damage by inhibiting STAT5-PGAM5-Drp1 signaling after BCAS. (**A**-**B**) Effects of MDL-800 treatment on the ultrastructure of mitochondria after BCAS in mice, as detected using electron microscopy (yellow pentagram represent mitochondria). MDL-800: SIRT6 agonist. (**C**-**D**) Effects of MDL-800 treatment on STAT5-PGAM5-Drp1 pathway after BCAS in mice, as detected using western blot ($n=6$ per group). (E-H) Effects of MDL-800 treatment on ATP level, ROS production, and mitochondrial complex I /II activities after BCAS in mice ($n=6$ per group). Data are presented as means ± SD. $^{*}P<0.05$, $^{**}P<0.01$, $^{***}P<0.001$

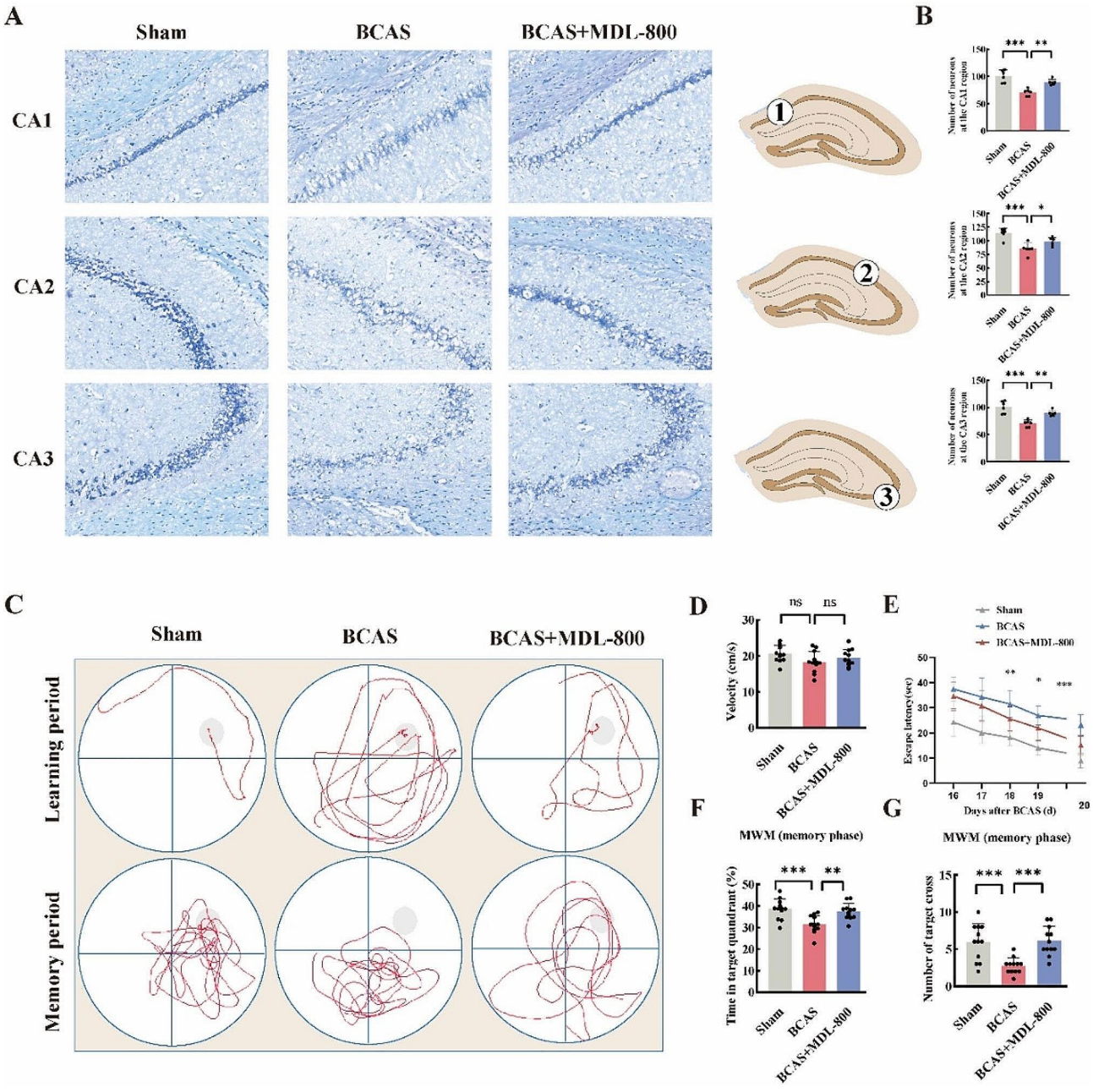

Fig. 5 SIRT6 prevents neuronal loss and cognitive deficit after chronic cerebral hypoperfusion. (**A**-**B**) Representative images and quantification illustrating Nissl positively stained neurons in hippocampal CA1, CA2, and CA3 regions in BCAS mice following MDL-800 treatment ($n = 6$ per group). (**C**-**G**) The animals' learning and memory functions were assessed by the Morris water maze test. (**C**) Representative swim paths. (**D**) Latency to escape in BCAS mice following MDL-800 treatment. ($n = 12$ per group). (**E**) Swimming speed of mice in each group. (**F**) The number of platform zone crossings. $n = 12$/group. (**G**) The time spent on the target platform zone. $n = 12$/group. ($n = 12$ per group). Data are presented as means ± SD. $^{*}P < 0.05$, $^{**}P < 0.01$, $^{***}P < 0.001$

demonstrated that Sirt6 expression possessed superior predictive ability for cognitive outcomes. Multivariate logistic regression analysis also identified Sirt6 expression as an independent influencing factor for cognitive outcomes in patients with asymptomatic carotid stenosis. Additional information regarding the baseline clinical characteristics of the study cohort can be found in Supplemental Table 1.

Discussion

In the present study, we made a noteworthy observation regarding the marked down-regulation of SIRT6 expression in BCAS mice exhibiting cognitive impairment. Our subsequent investigations revealed that Sirt6 deficiency further aggravated neuronal damage and cognitive deficits in the context of CCH. Conversely, activation of SIRT6 activity demonstrated its effectiveness

Table 1 Characteristics of the study patients

Variables	Study population ($n=164$)	Good outcome ($n=94$)	Poor outcome ($n=70$)	Crude OR (95% CI)	Crude *P* value	Adjusted OR (95% CI)	Adjusted *P* value
Demographics (age, mean ± SD; male, %)							
Sex							
Female	93(56.7%)	58(38.3%)	35(50%)	0.62(0.33,1.16)	0.136		
Male	71(43.3%)	36(61.7%)	35(50%)				
Age(years)							
< 60	72(43.9%)	54(57.4%)	18(25.7%)				
60–70	66(40.2%)	32(34.0%)	34(48.6%)	3.19(1.55,6.55)	0.002	2.74(1.09,6.91)	0.03
> 70	26(15.9%)	8(8.5%)	18(25.7%)	6.75(2.51,18.15)	< 0.001	9.96(2.47,40.22)	0.01
Clinical characteristics							
Education level(years)							
< 7	68(41.5%)	26(27.7%)	42(60%)				
7–9	69(42.1%)	46(48.9%)	23(32.9%)	0.31(0.15,0.63)	0.001		
> 9	27(16.5%)	22(23.4%)	5(7.1%)	0.14(0.05,0.42)	< 0.001		
Diabetes							
Yes	92(56.1%)	40(42.6%)	52(74.3%)	3.9(1.98,7.65)	< 0.001	3.7(1.50,9.12)	0.005
No	72(43.9%)	72(57.4%)	70(25.7%)				
Cerebrovascular disease							
Yes	66(40.2%)	31(33.0%)	35(50.0%)	2.03(1.08,3.84)	0.029	2.66(1.06,6.65)	0.04
No	98(59.8%)	63(67.0%)	35(50.0%)				
Residence location							
Rural	67(40.9%)	30(31.9%)	37(52.9%)	2.39(1.26,4.53)	0.007		
Urban	97(59.1%)	64(68.1%)	33(47.1%)				
Laboratory test (mean ± SD)							
WBC (10^9/L)	9.07(3.71)	9.47(3.72)	8.54(3.66)	0.93(0.86,1.02)	0.12		
AST (U/L)	34.34(8.82)	34.99(8.85)	34.45(8.77)	0.98(0.95,1.01)	0.27		
ALT(U/L)	31.08(8.84)	30.82(8.45)	31.42(9.38)	1.01(0.97,1.04)	0.67		
TC(mmol/L)	5.79(0.88)	5.84(0.88)	5.74(0.87)	088(0.62,1.25)	0.47		
TG(mmol/L)	3.86(0.76)	3.91(0.73)	3.78(0.81)	0.79(0.53,1.20)	0.27		
HDL(mmol/L)	1.65(0.46)	1.6(0.44)	1.65(0.49)	0.92(0.47,1.81)	0.81		
LDL(mmol/L)	2.99(0.73)	2.95(0.74)	3.03(0.73)	1.18(0.77,1.80)	0.45		
PLT(10^9/L)	219.33(31.15)	221.8(30.06)	216.00(32.5)	0.99(0.98,1.00)	0.24		
APTT (s)	26.23(4.81)	25.98(5.15)	26.58(4.30)	1.03(0.96,1.09)	0.42		
D-dimers	297.85(53.71)	300.9(51.67)	293.75(56.46)	0.99(0.99,1.00)	0.40		
Folate(μg/L)	20.85(14.65)	20.88(14.56)	20.81(14.88)	1.00(0.98,1.02)	0.98		
vitamin B12(μg/L)	361.39(279.52)	340.98(241.98)	388.79(322.99)	1.00(0.99,1.02)	0.28		
Hcy(μmol/L)	17.84(14.23)	15.62(11.53)	20.82(16.84)	1.03(1.00,1.06)	0.04	1.06(1.01,1.10)	0.004
Relative mRNA (Sirt6)	0.80(0.48)	1.00(0.50)	0.54(0.30)	0.039(0.01,0.13)	< 0.001	0.053(0.01,0.21)	< 0.001

Abbreviations: homocysteine (Hcy), white blood cells (WBC), aspartate aminotransferase (AST), alanine aminotransferase (ALT), total cholesterol (TC), Direct bilirubin(TG), Triglycerides (TG), high-density lipoprotein (HDL), low-density lipoprotein (HDL), activated partial thromboplastin time(APTT), Platelet(PLT).

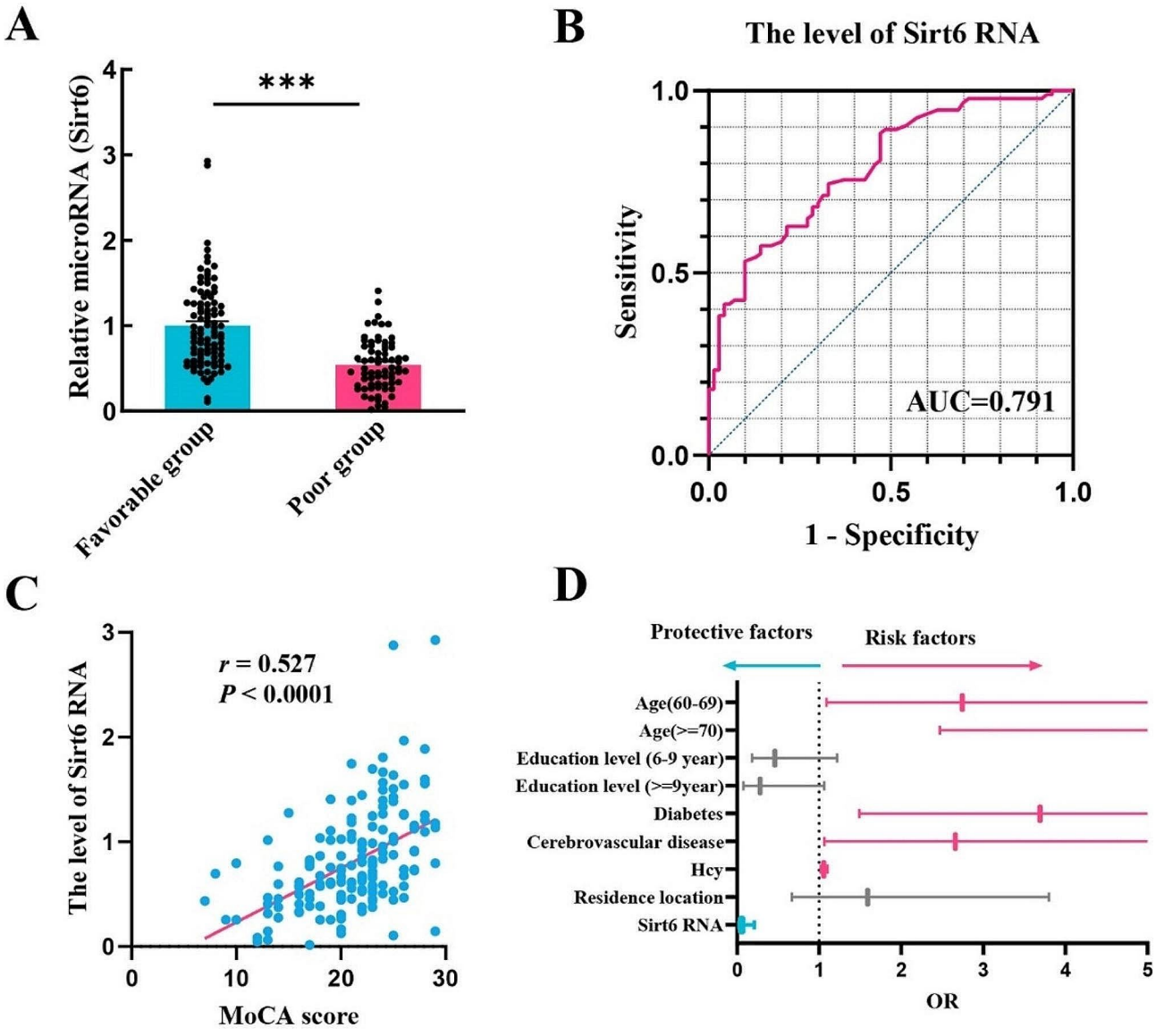

Fig. 6 SIRT6 gene expression in patients with asymptomatic carotid stenosis correlates with the cognitive outcome. (**A**) Sirt6 mRNA expression in PBMCs is higher in patients with unsatisfactory outcome compared to those in patients with satisfactory outcome ($P < 001$). Unsatisfactory outcome: MoCA score was less than 21. Satisfactory outcome: MoCA score was greater than or equal to 21. (**B**) ROC analysis of the discriminative ability of Sirt6 mRNA expression for unsatisfactory outcome in patients with asymptomatic carotid stenosis. Area under the curve (AUC): 0.791. (**C**) Linear correlation between Sirt6 mRNA expression and cognitive outcome assessed using MoCA scores in patients with asymptomatic carotid stenosis. *$P < 0.05$, **$P < 0.01$, ***$P < 0.01$

in mitigating neuronal loss and promoting neurological recovery. Mechanism-wise, SIRT6 exhibited neuroprotective effects, partially attributed to its ability to impede excessive mitochondrial fission through a STAT5-PGAM5-Drp1 dependent pathway. Additionally, we gathered compelling evidence demonstrating a correlation between monocyte SIRT6 gene expression in patients with asymptomatic carotid stenosis and cognitive outcomes. Collectively, our findings shed light on an undisclosed role of SIRT6 in safeguarding against CCH-induced cognitive impairment, while simultaneously uncovering a novel mechanistic pathway underlying its neuroprotective functions.

SIRT6 is an enzyme that relies on nicotinamide adenine dinucleotide+ (NAD+) for its functionality. It exhibits various activities, including histone 3 lysine 9 (H3K9) and histone 3 lysine 56 (H3K56) deacetylase, and acylase functions, all of which are involved in the regulation of numerous genes. SIRT6 has emerged as an intriguing target for various conditions, including CNS disorders, cancer, aging and metabolic disorders. For instance, SIRT6 has been implicated in the modulation of adult hippocampal neurogenesis, thus holding potential therapeutic

implications for cognitive deficits-related diseases [39, 40]. But the role of SIRT6 in VaD remains unexplored. Herein, we observed a significant reduction in SIRT6 protein expression levels in a BCAS mouse model, suggesting a potential critical involvement of SIRT6 in the pathophysiology of VaD. To gain deeper insights into the role of SIRT6 in VaD, we generated neuron-specific Sirt6 knockout mice. Remarkably, our findings demonstrated that Sirt6 knockout worsened the learning and memory abilities of mice following BCAS, whereas treatment with a SIRT6 agonist ameliorated cognitive impairment. Furthermore, Sirt6 was found to attenuate neuronal loss induced by BCAS, which was consistent with the observed improvement in cognitive function. In order to increase the translational relevance of our preclinical findings, we analysed SIRT6 expression levels in monocytes of patients with asymptomatic carotid stenosis. And we found that SIRT6 expression were significantly higher in patients showing cognitive improvement when compared to the patients with unfavourable outcome. Above all, we discovered an unidentified role of SIRT6 in preventing CCH-induced cognitive impairment.

Recent studies have indicated that dysfunction in mitochondrial dynamics plays a significant role in both acute brain injury and neurodegenerative diseases, including cerebral ischemic stroke, traumatic brain injury, Alzheimer's disease, Parkinson's disease, and amyotrophic lateral sclerosis. Mitochondrial dynamics involve fusion and fission processes that intricately regulate the morphology and function of mitochondria. The regulation of mitochondrial fission is primarily dependent on Drp1, whose altered activity has been implicated in the pathogenesis of central nervous system disorders. The phosphorylation of Drp1 at S637 has recently emerged as a critical factor in the development of neural system disorders and neurodegenerative diseases. For instance, phosphorylation of Drp1 has been shown to increase neuronal apoptosis, making neurons more vulnerable to Aβ toxicity in an Alzheimer's disease mouse model [41]. Furthermore, phosphorylation of Drp1 affects the maturation of neurons and the maintenance of differentiation and stemness in neural system progenitor cells. In our study, we observed misshapen mitochondria lacking their characteristic internal structure in the BCAS group. Mechanistically, although the total protein level of Drp1 did not significantly change after BCAS in mice, the phosphorylation level at S637 was markedly decreased, leading to the translocation of DRP1 to the mitochondrial membrane and excessive mitochondrial fission. However, SIRT6 treatment enhanced the phosphorylation of Drp1 at S637 by inhibiting the STAT5-PGAM5 pathway, which was significantly activated after BCAS, thereby alleviating mitochondrial morphological loss. Furthermore, along with the improvement in mitochondrial morphology, we found that SIRT6 significantly restored ATP production, enhanced the activities of the electron transport chain, and reduced the production of reactive oxygen species after BCAS. Thus, we concluded that SIRT6 could preserve mitochondrial dynamics and enhance mitochondrial biogenesis, which in turn reduces the BCAS-mediated neuronal damage and cognitive deficits.

However, our study has certain limitations that need to be acknowledged. Firstly, it is important to recognize that the experimental models employed in young, healthy rodents may not fully replicate the injury scenario observed in clinical practice among VaD patients. These patients often exhibit a diverse range of pathophysiological factors, thereby necessitating future research to explore additional variables such as age, sex, genetic background, and comorbidities. Secondary, it should be noted that the neuroprotective effects of SIRT6 may extend beyond the observations made in this study. For instance, SIRT6 may potentially play a role in regulating autophagy, thereby influencing neuronal loss. As a result, it is worthwhile to further investigate other potential mechanisms of action for SIRT6 in the BCAS model in future studies.

In conclusion, our findings demonstrate that SIRT6 confers protection against cognitive impairment induced by CCH. One possible molecular mechanism underlying this effect is that SIRT6 facilitates the remodeling of mitochondrial dynamics in a STAT5-PGAM5-Drp1 dependent manner. Consequently, targeting neuronal SIRT6 may hold promise as a therapeutic approach for ameliorating cognitive impairment following CCH.

Abbreviations

VaD	Vascular dementia
CCH	Chronic cerebral hypoperfusion
SIRT6	Sirtuin 6
BCAS	Bilateral common carotid artery stenosis
CNS	Central nervous system
ATP	Adenosine triphosphate
PBMCs	Peripheral blood mononuclear cells
ROC	Receiver operating characteristic

Supplementary Information

The online version contains supplementary material available at https://doi.org/10.1186/s12967-024-05566-0.

Supplementary Material 1

Funding

This work was supported by the National Natural Science Foundation of China (No.81571215) and (No.82371384), and the Scientific Research Fund Project of the Hebei Provincial Health and Family Planning Commission (No. 20240113), and the Natural Science Foundation of Hebei Province (H202306146).

Data availability

The datasets used and/or analyzed during the current study are available from the corresponding author on reasonable request.

Declarations

Ethical approval
The animal study protocol was approved by the Ethics Committee of the Air Force Medical University. All experimental procedures adhered strictly to the guidelines outlined in the National Institutes of Health Guide for the Care and Use of Laboratory Animals, thereby ensuring the welfare and ethical treatment of the animal subjects.

Competing interests
The authors have declared that no conflict of interest exists.

Received: 7 June 2024 / Accepted: 1 August 2024
Published online: 25 August 2024

References

1. O'Brien JT, Thomas A. Vascular dementia. Lancet (London England). 2015;386(10004):1698–706.
2. Rajeev V, Fann DY, Dinh QN, Kim HA, De Silva TM, Lai MKP, Chen CL, Drummond GR, Sobey CG, Arumugam TV. Pathophysiology of blood brain barrier dysfunction during chronic cerebral hypoperfusion in vascular cognitive impairment. Theranostics. 2022;12(4):1639–58.
3. Poh L, Sim WL, Jo DG, Dinh QN, Drummond GR, Sobey CG, Chen CL, Lai MKP, Fann DY, Arumugam TV. The role of inflammasomes in vascular cognitive impairment. Mol Neurodegeneration. 2022;17(1):4.
4. Inoue Y, Shue F, Bu G, Kanekiyo T. Pathophysiology and probable etiology of cerebral small vessel disease in vascular dementia and Alzheimer's disease. Mol Neurodegeneration. 2023;18(1):46.
5. Zhao Y, Zhang J, Zheng Y, Zhang Y, Zhang XJ, Wang H, Du Y, Guan J, Wang X, Fu J. NAD(+) improves cognitive function and reduces neuroinflammation by ameliorating mitochondrial damage and decreasing ROS production in chronic cerebral hypoperfusion models through Sirt1/PGC-1α pathway. J Neuroinflamm. 2021;18(1):207.
6. Han B, Jiang W, Liu H, Wang J, Zheng K, Cui P, Feng Y, Dang C, Bu Y, Wang QM, et al. Upregulation of neuronal PGC-1α ameliorates cognitive impairment induced by chronic cerebral hypoperfusion. Theranostics. 2020;10(6):2832–48.
7. Ji ML, Jiang H, Li Z, Geng R, Hu JZ, Lin YC, Lu J. Sirt6 attenuates chondrocyte senescence and osteoarthritis progression. Nat Commun. 2022;13(1):7658.
8. Wu X, Liu H, Brooks A, Xu S, Luo J, Steiner R, Mickelsen DM, Moravec CS, Jeffrey AD, Small EM, et al. SIRT6 mitigates heart failure with preserved ejection fraction in diabetes. Circul Res. 2022;131(11):926–43.
9. Li W, Feng W, Su X, Luo D, Li Z, Zhou Y, Zhu Y, Zhang M, Chen J, Liu B et al. SIRT6 protects vascular smooth muscle cells from osteogenic transdifferentiation via Runx2 in chronic kidney disease. J Clin Investig 2022, 132(1).
10. Khan D, Ara T, Ravi V, Rajagopal R, Tandon H, Parvathy J, Gonzalez EA, Asirvatham-Jeyaraj N, Krishna S, Mishra S, et al. SIRT6 transcriptionally regulates fatty acid transport by suppressing PPARγ. Cell Rep. 2021;35(9):109190.
11. Tasselli L, Zheng W, Chua KF. SIRT6: novel mechanisms and links to Aging and Disease. Trends Endocrinol Metab. 2017;28(3):168–85.
12. Liberale L, Gaul DS, Akhmedov A, Bonetti NR, Nageswaran V, Costantino S, Pahla J, Weber J, Fehr V, Vdovenko D, et al. Endothelial SIRT6 blunts stroke size and neurological deficit by preserving blood-brain barrier integrity: a translational study. Eur Heart J. 2020;41(16):1575–87.
13. Kaluski S, Portillo M, Besnard A, Stein D, Einav M, Zhong L, Ueberham U, Arendt T, Mostoslavsky R, Sahay A, et al. Neuroprotective functions for the histone deacetylase SIRT6. Cell Rep. 2017;18(13):3052–62.
14. Smirnov D, Eremenko E, Stein D, Kaluski S, Jasinska W, Cosentino C, Martinez-Pastor B, Brotman Y, Mostoslavsky R, Khrameeva E, et al. SIRT6 is a key regulator of mitochondrial function in the brain. Cell Death Dis. 2023;14(1):35.
15. Zhao J, Qu D, Xi Z, Huan Y, Zhang K, Yu C, Yang D, Kang J, Lin W, Wu S, et al. Mitochondria transplantation protects traumatic brain injury via promoting neuronal survival and astrocytic BDNF. Transl Res. 2021;235:102–14.
16. Anastasia I, Ilacqua N, Raimondi A, Lemieux P, Ghandehari-Alavijeh R, Faure G, Mekhedov SL, Williams KJ, Caicci F, Valle G, et al. Mitochondria-rough-ER contacts in the liver regulate systemic lipid homeostasis. Cell Rep. 2021;34(11):108873.
17. Noterman MF, Chaubey K, Lin-Rahardja K, Rajadhyaksha AM, Pieper AA, Taylor EB. Dual-process brain mitochondria isolation preserves function and clarifies protein composition. Proc Natl Acad Sci USA 2021, 118(11).
18. Tukacs V, Mittli D, Hunyadi-Gulyás É, Hlatky D, Medzihradszky KF, Darula Z, Nyitrai G, Czurkó A, Juhász G, Kardos J, et al. Chronic Cerebral Hypoperfusion-Induced Disturbed Proteostasis of Mitochondria and MAM is reflected in the CSF of rats by Proteomic Analysis. Mol Neurobiol. 2023;60(6):3158–74.
19. Feng T, Yamashita T, Zhai Y, Shang J, Nakano Y, Morihara R, Fukui Y, Hishikawa N, Ohta Y, Abe K. Chronic cerebral hypoperfusion accelerates Alzheimer's disease pathology with the change of mitochondrial fission and fusion proteins expression in a novel mouse model. Brain Res. 2018;1696:63–70.
20. Su SH, Wu YF, Wang DP, Hai J. Inhibition of excessive autophagy and mitophagy mediates neuroprotective effects of URB597 against chronic cerebral hypoperfusion. Cell Death Dis. 2018;9(7):733.
21. Ni HM, Williams JA, Ding WX. Mitochondrial dynamics and mitochondrial quality control. Redox Biol. 2015;4:6–13.
22. König T, Nolte H, Aaltonen MJ, Tatsuta T, Krols M, Stroh T, Langer T, McBride HM. MIROs and DRP1 drive mitochondrial-derived vesicle biogenesis and promote quality control. Nat Cell Biol. 2021;23(12):1271–86.
23. Wu L, Wang L, Du Y, Zhang Y, Ren J. Mitochondrial quality control mechanisms as therapeutic targets in doxorubicin-induced cardiotoxicity. Trends Pharmacol Sci. 2023;44(1):34–49.
24. Jiang Y, Krantz S, Qin X, Li S, Gunasekara H, Kim YM, Zimnicka A, Bae M, Ma K, Toth PT, et al. Caveolin-1 controls mitochondrial damage and ROS production by regulating fission - fusion dynamics and mitophagy. Redox Biol. 2022;52:102304.
25. Kleele T, Rey T, Winter J, Zaganelli S, Mahecic D, Perreten Lambert H, Ruberto FP, Nemir M, Wai T, Pedrazzini T, et al. Distinct fission signatures predict mitochondrial degradation or biogenesis. Nature. 2021;593(7859):435–9.
26. Kraus F, Roy K, Pucadyil TJ, Ryan MT. Function and regulation of the divisome for mitochondrial fission. Nature. 2021;590(7844):57–66.
27. Calvo-Rodriguez M, Bacskai BJ. Mitochondria and Calcium in Alzheimer's Disease: from cell signaling to neuronal cell death. Trends Neurosci. 2021;44(2):136–51.
28. Lian WW, Zhou W, Zhang BY, Jia H, Xu LJ, Liu AL, Du GH. DL0410 ameliorates cognitive disorder in SAMP8 mice by promoting mitochondrial dynamics and the NMDAR-CREB-BDNF pathway. Acta Pharmacol Sin. 2021;42(7):1055–68.
29. Wang J, Fröhlich H, Torres FB, Silva RL, Poschet G, Agarwal A, Rappold GA. Mitochondrial dysfunction and oxidative stress contribute to cognitive and motor impairment in FOXP1 syndrome. Proc Natl Acad Sci USA 2022, 119(8).
30. Liu Y, Chu JMT, Ran Y, Zhang Y, Chang RCC, Wong GTC. Prehabilitative resistance exercise reduces neuroinflammation and improves mitochondrial health in aged mice with perioperative neurocognitive disorders. J Neuroinflamm. 2022;19(1):150.
31. Poh L, Fann DY, Wong P, Lim HM, Foo SL, Kang SW, Rajeev V, Selvaraji S, Iyer VR, Parathy N, et al. AIM2 inflammasome mediates hallmark neuropathological alterations and cognitive impairment in a mouse model of vascular dementia. Mol Psychiatry. 2021;26(8):4544–60.
32. Miao W, Jiang L, Xu F, Lyu J, Jiang X, He M, Liu Y, Yang T, Leak RK, Stetler RA, et al. Adiponectin ameliorates hypoperfusive cognitive deficits by boosting a neuroprotective microglial response. Prog Neurobiol. 2021;205:102125.
33. Wu X, Cui W, Guo W, Liu H, Luo J, Zhao L, Guo H, Zheng L, Bai H, Feng D, et al. Acrolein aggravates secondary Brain Injury after Intracerebral Hemorrhage through Drp1-Mediated mitochondrial oxidative damage in mice. Neurosci Bull. 2020;36(10):1158–70.
34. Wu X, Luo J, Liu H, Cui W, Guo W, Zhao L, Guo H, Bai H, Guo K, Feng D, et al. Recombinant adiponectin peptide promotes neuronal survival after intracerebral haemorrhage by suppressing mitochondrial and ATF4-CHOP apoptosis pathways in diabetic mice via Smad3 signalling inhibition. Cell Prolif. 2020;53(2):e12759.
35. Cui W, Wu X, Shi Y, Guo W, Luo J, Liu H, Zheng L, Du Y, Wang P, Wang Q, et al. 20-HETE synthesis inhibition attenuates traumatic brain injury-induced mitochondrial dysfunction and neuronal apoptosis via the SIRT1/PGC-1α pathway: a translational study. Cell Prolif. 2021;54(2):e12964.
36. Aczél T, Körtési T, Kun J, Urbán P, Bauer W, Herczeg R, Farkas R, Kovács K, Vásárhelyi B, Karvaly GB, et al. Identification of disease- and headache-specific mediators and pathways in migraine using blood transcriptomic and metabolomic analysis. J Headache Pain. 2021;22(1):117.
37. Song X, Liu Y, Pu J, Gui S, Zhong X, Chen X, Chen W, Chen X, Chen Y, Wang H, et al. Transcriptomics Analysis reveals Shared pathways in Peripheral Blood mononuclear cells and brain tissues of patients with Schizophrenia. Front Psychiatry. 2021;12:716722.
38. Mahapatra G, Gao Z, Bateman JR 3rd, Lockhart SN, Bergstrom J, DeWitt AR, Piloso JE, Kramer PA, Gonzalez-Armenta JL, Amick KA, et al. Blood-based bioenergetic profiling reveals differences in mitochondrial function associated

with cognitive performance and Alzheimer's disease. Alzheimer's Dement J Alzheimer's Assoc. 2023;19(4):1466–78.
39. Matsuno H, Tsuchimine S, Fukuzato N, O'Hashi K, Kunugi H, Sohya K. Sirtuin 6 is a regulator of dendrite morphogenesis in rat hippocampal neurons. Neurochem Int. 2021;145:104959.
40. Okun E, Marton D, Cohen D, Griffioen K, Kanfi Y, Illouz T, Madar R, Cohen HY. Sirt6 alters adult hippocampal neurogenesis. PLoS ONE. 2017;12(6):e0179681.
41. Yuan Y, Chen J, Ge X, Deng J, Xu X, Zhao Y, Wang H. Activation of ERK-Drp1 signaling promotes hypoxia-induced Aβ accumulation by upregulating mitochondrial fission and BACE1 activity. FEBS open bio. 2021;11(10):2740–55.

Publisher's Note